Coverage Analysis of a THz Cellular Network in the Presence of Scatterers

Kaushlendra Pandey, Aman Kumar Pandey, Abhishek K. Gupta, Harpreet S. Dhillon

***Abstract*—In this paper, we present a comprehensive analytical framework for the system level analysis of THz cellular networks, which incorporates all key features of THz propagation, including blocking, directionality and scattering. This framework is particularly novel from the perspective of including the effect of scattering that has been largely ignored in such analyses thus far. We model the locations of the THz base-stations (BSs) as a homogeneous Poisson point process (PPP) and users (UEs) as another independent point process (PP). Further, the blockages and scatterers are modeled using a Boolean process and an independent PPP, respectively. The framework also incorporates distinction of line-of-sight (LOS), non-line-of-sight (NLOS) links, a realistic bounded path-loss model with absorption losses, and antenna directivity. Using the proposed framework, we first characterize the interference caused by BSs and scatterers via its Laplace transform (LT). We then derive the SINR (signal to interference plus noise ratio) coverage probability. With the help of a dummy exponential random variable (RV), we also derive the exact mean SINR. Our analysis concretely demonstrates that the scatterers have a significant impact on the coverage probability. Further, our results show that the coverage probability does not always increase with the increasing density of THz BSs.**

I. Introduction

Enormous unexplored spectrum in the sub-THz and THz (collectively termed as THz in this paper) range provides an appealing solution for supporting ultra-high data rates required in emerging applications, such as virtual and augmented reality, metaverse, and 3D gaming [1]. However, propagation characteristics in this range are far less favorable because of higher propagation losses, including losses due to molecular absorption, higher sensitivity to blockages, and a pronounced effect of scattering. As a result, THz wireless links are often considered significantly less reliable than the lower frequencies. However, in order to present an accurate picture about their performance, we need a comprehensive framework that jointly models the locations of wireless nodes as well as the aforementioned propagation effects impacting the performance, which is the main goal of this paper.

Related work: Given the popularity of using stochastic geometry (SG) for the modeling and analysis of a variety of wireless networks, it is not surprising that it has also found use in the analysis of THz networks [2]–[8]. The analysis of SINR distribution at the lower frequencies is facilitated by including an exponential fading gain term for the serving link (justified by making a Rayleigh fading assumption), which allows one to write the distribution of SINR in terms of the Laplace transform of interference, thereby simplifying the problem significantly. However, the absence of fading at the THz frequencies means that a similar approach cannot be directly extended to THz, which is the main technical challenge in this analysis. This has been handled in the THz literature using different approaches, some of which are discussed next. In [2], authors have computed the moments of interference and SINR for a simplified model of THz ad-hoc network by fitting a log-logistic distribution to the interference (to simplify the analysis). The work was extended in [3] to include blockages and antenna directivity. In [4] authors computed the mean interference and the outage probability for a dense THz network by modeling the BSs location as a PPP (while ignoring the impact of blockages and scatterers). In [5], the authors used Talbot's technique to invert the LTs of interference to get the probability density function (PDF) of the interference. The authors in [6] studied the rate coverage probability and interference for dense THz networks and coexisting RF with dense THz networks. In [7], the authors analyzed the coverage probability for a heterogeneous network. In [8], coverage probability for a 3D THz network is studied.

Even though these works have provided useful design insights, a comprehensive framework that incorporates the effect of *all* key THz propagation characteristics has eluded us. In particular, all these works have failed to incorporate the impact of scattering in the analysis. Since scattering is significant at THz frequencies, it is expected that scattered power from various scatterers present in the environment may lead to non-negligible interference at the user.

Contribution: In this paper, we present a comprehensive analytical framework to analyze a THz cellular network which incorporates the impact of blocking, directionality and scattering. In particular, the inclusion of scattering in this analysis is a key novelty of our work. This framework models THz BSs as a homogeneous PPP, UEs as independent PP, blockages as a Boolean process, and scatterers as a PPP. It also incorporates the distinction of LOS/NLOS links, a realistic bounded path-loss model with absorption losses, and antenna directivity. Using the proposed framework, we derive the closed form expression for SINR coverage probability. With the help of a dummy fading coefficient, we also present the mean SINR expression. Finally, we investigate the impact of scatterer density and BS densification with the help of numerical results.

Notation: The notation $\mathbf{x}$ represents a 2D vector, and its norm is $\|\mathbf{x}\| = x$. The origin is denoted by $\mathbf{o}$. The cumulative distribution function (CDF), and PDF of RV X are denoted

K. Pandey, A. K. Pandey and A. K. Gupta are with IIT Kanpur, India, 208016. Email:{kpandey, amanpandey20, gkrabhi}@iitk.ac.in. H. S. Dhillon is with Virginia Tech, Blacksburg, VA 24061 (Email: hdhillon@vt.edu). H. S. Dhillon gratefully acknowledges the support of the US National Science Foundation (Grants CNS-1923807 and ECCS-2030215).

by $F_X(x)$, and $f_X(x)$, respectively. The expected value of a RV X is denoted as $\mathbb{E}[X]$. The notation c stands for the speed of light. For a non negative random number X, its mean is given as

$$\mathbb{E}[X] = \int_{\tau=0}^{\infty} \mathbb{P}\left(X > \tau\right) \mathrm{d}\tau. \tag{1}$$

The notation $\ell(\cdot)$ denotes the path loss-model and $\mathsf{W}_0(\cdot)$ is the $\mathsf{LambertW}(\cdot)$ function [9].

II. System Model

Network model: We consider a THz network consisting of multiple THz BSs with locations distributed as a PPP $\Phi = \{\mathbf{z}_i, \forall i \in \mathbb{N}\}$ with density λ_{b}. Further the locations of UEs are distributed as a stationary PP Φ_{u} with density λ_{u}. Owing to its stationarity, we focus on the typical user located at the origin.

Modeling of blockages: Blockages are modeled using a Boolean process [10]. Under this model, a BS located at a distance z from the user is LOS with probability $p_{\mathrm{b}}(z) = e^{-\beta z}$, where β is a constant dependent on the density and size of blockages. For tractability, we assume that the blockages affect each link independently. Hence, BSs can be divided into two point processes, one consisting of LOS BSs and the other consisting of NLOS BSs. Due to the independent thinning theorem [11], each of these is a PPP and denoted by Φ_{L} and Φ_{N}, respectively. Their densities are $\lambda_{\mathrm{L,b}}(z) = \lambda_{\mathrm{b}} e^{-\beta z}$ and $\lambda_{\mathrm{N,b}}(z) = \lambda_{\mathrm{b}}(1 - e^{-\beta z})$, respectively.

Modeling of scatterers: In this paper, we also incorporate the impact of the interference power arriving from the scatterers, which is a key novelty of our analysis. To account for this effect, we model the scatterers as a PPP Φ_{s} with density λ_{s}. The signal transmitted by each LOS BS is scattered around by the scatterers. Therefore, a fraction of the signal scattered by each LOS scatterer acts as interference at the typical user. Note that due to very high path-loss for NLOS links [1], we ignore the impact of NLOS links in this work similar to past works [4], [6], [12], [13]. Let $\Phi_{\mathrm{s}}^{'} = \{\mathbf{y}_i, \forall i \in \mathbb{N}\}$ denote the PP consisting of all scatterers that are in LOS to the typical user. Similar to LOS BSs, the LOS scatterers also form a PPP with density $\lambda_{\mathrm{s}} e^{-\beta y}$. The fraction of power scattered to the incident power is characterized by the square of the scattering coefficient S [14]. We assume that S is constant for all scatterers, however, it can be easily extended to scatterers with different values of S.

Antenna modeling: UEs and BSs are outfitted with directional antennas. The directivity of an antenna (transmitter or receiver) can be modeled by the widely used sector model [15]. Hence, the antenna gain at the device q ($\mathrm{q} \in \{\mathrm{t}, \mathrm{r}\}$) in the direction $\tilde{\beta}$ is given as

$$g_{\mathrm{q}}(\tilde{\beta}) = \begin{cases} \mathrm{G}_{\mathrm{m,q}}, & |\tilde{\beta}| \leq \phi_{\mathrm{q}}/2 \\ \mathrm{G}_{\mathrm{s,q}}, & \text{otherwise} \end{cases}, \tag{2}$$

where $\mathrm{G}_{\mathrm{m,q}}$ and $\mathrm{G}_{\mathrm{s,q}}$ denote the main and the side lobe and ϕ_q is the antenna beamwidth. Further, $\tilde{\beta} \in [-\pi, \pi)$ denotes the angle between the desired direction and the antenna orientation and q can be t or r representing the transmit and receiver end, respectively.

TABLE I
Probability distribution of directivity gain G_{z_i}.

Gain (G) values	**Corresponding probability**
$\mathrm{G}_1 = \mathrm{G}_{\mathrm{m,t}}\mathrm{G}_{\mathrm{m,r}}$	$\mathrm{p}_1 = \mathrm{p}_{\mathrm{t}}\mathrm{p}_{\mathrm{r}}$
$\mathrm{G}_2 = \mathrm{G}_{\mathrm{m,t}}\mathrm{G}_{\mathrm{s,r}}$	$\mathrm{p}_2 = \mathrm{p}_{\mathrm{t}}(1 - \mathrm{p}_{\mathrm{r}})$
$\mathrm{G}_3 = \mathrm{G}_{\mathrm{s,t}}\mathrm{G}_{\mathrm{m,r}}$	$\mathrm{p}_3 = (1 - \mathrm{p}_{\mathrm{t}})\mathrm{p}_{\mathrm{r}}$
$\mathrm{G}_4 = \mathrm{G}_{\mathrm{s,t}}\mathrm{G}_{\mathrm{s,r}}$	$\mathrm{p}_4 = (1 - \mathrm{p}_{\mathrm{t}})(1 - \mathrm{p}_{\mathrm{r}})$

Path loss model: To keep the analysis general and realistic, we consider the bounded path loss model [16]. Hence, the path loss suffered by a link of length z is given as

$$\ell(z) = \gamma \min(1, z^{-\alpha_{\mathrm{L}}} \exp(-\kappa_f z)),$$

where $\gamma = p_{\mathrm{t}} c^2/(4\pi f)^2$ denotes the near field gain, κ_f is the absorption coefficient which depends on the composition of the atmospheric gas molecules and the frequency of the signal [17], α_{L} is path-loss exponent and p_{t} is the transmit power. Since THz links do not suffer from fading, it will not appear in the received power equations, which complicates the analysis significantly.

Cell association model and SINR: We consider the average power based association where each user connects to the closest LOS BS as its serving BS. Let us denote this BS as $\mathbf{z}_{\mathrm{o}}$. The rest of the LOS BSs act as interferers. The interference from these LOS BSs is given as

$$I_{\mathrm{b}} = \sum_{\mathbf{z}_i \in \Phi_{\mathrm{L}}, \mathbf{z}_i \neq \mathbf{z}_{\mathrm{o}}} \mathrm{G}_{z_i} \ell(z_i). \tag{3}$$

Here, G_{z_i} denotes the total (transmit and receive) antenna gain for the link between the BS at z_i and the typical user. Each BS aligns its antenna towards its associated user and vice-versa. Assuming that this user is uniformly located around its associated BS, G_{z_i} is a RV which can take four values with certain probabilities as given in TABLE I. Note that in TABLE I, $\mathrm{p}_{\mathrm{t}} = \frac{\phi_{\mathrm{t}}}{2\pi}$ and $\mathrm{p}_{\mathrm{r}} = \frac{\phi_{\mathrm{r}}}{2\pi}$ denote the probability of having maximum gain from each BS from transmitter and receiver antennas, respectively. Apart from the interference from these BSs, the power scattered from scatterers also contribute to the total interference. The interference from scatterers depends on the power $\mathrm{P}_{\mathrm{s},i}$ incident on each scatterer $\mathbf{y}_i$ transmitted from all LOS BSs. In particular, the interference at the typical user due to all the scatterers is given as

$$I_{\mathrm{s}} = \sum_{\mathbf{y}_i \in \Phi_{\mathrm{s}}^{'}} S^2 \mathrm{P}_{\mathrm{s},i} g_{\mathrm{r},i} \ell(y_i), \tag{4}$$

where antenna gain $g_{\mathrm{r},i} = \{\mathrm{G}_{\mathrm{m,r}}, \mathrm{G}_{\mathrm{s,r}}\}$ with probabilities p_{r} and $(1 - \mathrm{p}_{\mathrm{r}})$, respectively.

Let R_{o} be the distance between the closest LOS BS and the typical user *i.e.* $R_{\mathrm{o}} = \|\mathbf{z}_{\mathrm{o}}\|$. Since the directivity gain for the serving link is $\mathrm{G}_{z_o} = \mathrm{G}_{m,\mathrm{t}}\mathrm{G}_{\mathrm{m,r}}$, the signal power from the serving BS is

$$S(R_{\mathrm{o}}) = \mathrm{G}_{\mathrm{m,t}}\mathrm{G}_{\mathrm{m,r}} \ell(R_{\mathrm{o}}). \tag{5}$$

Hence, the SINR at the typical user is

$$\text{SINR} = \frac{S(R_\text{o})}{I_\text{b} + I_\text{s} + N_\text{o}}, \tag{6}$$

where N_o denotes noise. In the next section, we will study the THz network performance in terms of the SINR coverage probability which is defined as the probability that the SINR at the typical user is above threshold τ, *i.e.* $\text{p}_\text{c}(\tau) = \mathbb{P}[\text{SINR} > \tau]$.

III. Coverage Analysis

We first derive expressions for intermediate metrics that are required to derive the coverage probability. This includes the serving BS's distance distribution and the LT of the distributions of the powers of both types of interfering signals.

A. Serving BS distance distribution

The PDF of the serving BS's distance R_o is given as [18]

$$f_{R_\text{o}}(r) = 2\pi\lambda_\text{b} r e^{-\beta r} \exp\left(-\frac{2\pi\lambda_\text{b}}{\beta^2}\left(1 - e^{-\beta r}(\beta r + 1)\right)\right). \tag{7}$$

B. LT of the interference

We now derive the LT of the interference from the LOS BSs conditioned on the serving distance R_o which is given in the following lemma.

Lemma 1. *The LT of interference I_b from LOS BSs at the typical user given the distance R_o from its serving BS is written as (for proof see Appendix A.)*

$$\mathcal{L}_{I_\text{b}|R_\text{o}}(s) = \exp\Bigg(-\pi\lambda_\text{b}\times \sum_{n=1}^{4} \text{p}_n \int_1^\infty \left(1 - e^{-s\text{G}_n \ell(R_\text{o}\sqrt{t})}\right) e^{-\beta R_\text{o}\sqrt{t}} R_\text{o}^2 \text{d}t\Bigg), \tag{8}$$

where p_n's are provided in TABLE I.

Now, we will determine the LT of interference from the LOS scatterers. To simplify the analysis (largely because of space constraints), we approximate the total power falling on the typical scatterer with its mean P_s (*i.e.* $\text{P}_{\text{s},i} = \text{P}_\text{s}$, $\forall \mathbf{y}_i \in \Phi_\text{s}^{'}$), which is given in the following lemma.

Lemma 2. *The average power incident on the typical scatterer from all LOS BSs is (for proof see Appendix B.)*

$$\text{P}_\text{s} = 2\pi\lambda_\text{b} g_\text{t}^1 \frac{A_\text{s}}{4\pi}\left[\int_{z=0}^\infty \ell(z) e^{-\beta z} z \text{d}z\right], \tag{9}$$

where A_s is the mean effective scatterer area [1] and $g_\text{t}^1 = \text{G}_{\text{m,t}}\text{p}_\text{t} + \text{G}_{\text{s,t}}(1 - \text{p}_\text{t})$ is the mean of the transmit antenna gain from the typical BS.

Now, the scattered power from each of the scatterers reaching the typical user acts as interference whose LT is given in the following Lemma. Note that the typical user can receive this power via either main or side lobe depending on its orientation with respect to each scatterer's location.

Lemma 3. *The LT $\mathcal{L}_{I_\text{s}}(s)$, of the interference due to LOS scatterers is (for proof see Appendix C) $\mathcal{L}_{I_\text{s}}(s) =$*

$$\exp\left(-2\pi\lambda_s \sum_{j=1}^{2} \text{p}_{\text{r},j} \int_{y=0}^\infty \left(1 - e^{-sh_j(y)}\right) e^{-\beta y} y \text{d}y\right), \tag{10}$$

where $h_1(y) = \text{P}_\text{s} S^2 \text{G}_{\text{m,r}} \ell(y)$ and $h_2(y) = \text{P}_\text{s} S^2 \text{G}_{\text{s,r}} \ell(y)$ with probabilities $\text{p}_{\text{r},1} = \text{p}_\text{r}$, $\text{p}_{\text{r},2} = (1 - \text{p}_\text{r})$ respectively.

Equipped with these two LT expressions, we now calculate the coverage probability for the typical user. Note that due to absence of the fading, the analysis is in general more difficult than lower frequency counterpart. In the proof of the following, we utilize Gil-Pelaez lemma [19]. Please see Appendix D for the complete proof.

Theorem 1. *The coverage probability $\text{p}_\text{c}(\tau)$ of the typical user in the THz network under the impact of scattering is*

$$\text{p}_\text{c}(\tau) = \frac{1}{2} + \frac{1}{\pi} \times \int_0^\infty \mathbb{E}_{R_\text{o}}\left[H(R_\text{o}, \tau) \times \sin\left(uS(R_\text{o}) - \Theta(R_\text{o}, \tau) - u\tau N_\text{o}\right)\right] \frac{\text{d}u}{u} \tag{11}$$

where $S(R_\text{o})$ is provided in (5)*,*

$$H(R_\text{o}, \tau) = \exp\Bigg(-\pi\lambda_\text{b} \sum_{n=1}^{4} \text{p}_n \times \int_{t=1}^\infty \left(1 - \cos\left(u\tau \text{G}_n \ell(R_\text{o}\sqrt{t})\right)\right) e^{-\beta R_\text{o}\sqrt{t}} R_\text{o}^2 \text{d}t - 2\pi\lambda_\text{s} \sum_{j=1}^{2} \text{p}_j \int_{y=0}^\infty \left(1 - \cos\left(u\tau h_j(y)\right)\right) e^{-\beta y} y \text{d}y\Bigg), \text{ and}$$

$$\Theta(R_\text{o}, \tau) = \sum_{n=1}^{4} \text{p}_n \pi\lambda_\text{b} \int_{t=1}^\infty \sin\left(u\tau \text{G}_n \ell(R_\text{o}\sqrt{t})\right) e^{-\beta R_\text{o}\sqrt{t}} \times R_\text{o}^2 \text{d}t + \sum_{j=1}^{2} \text{p}_j 2\pi\lambda_\text{s} \int_{y=0}^\infty \sin(u\tau h_j(y)) e^{-\beta y} y \text{d}y.$$

For the noise limited regime, the above can be simplified to give the following.

Corollary 1.1. *The coverage probability for noise limited regime i.e if we ignore the interference from the scatterers and BSs ($I_\text{b} = 0$, $I_\text{s} = 0$), is given as*

$$\text{p}_\text{c}(\tau) = \int_\rho^\infty f_{R_\text{o}}(r_\text{o}) \text{d}r_\text{o}, \tag{12}$$

where ρ is

$$= \max\left(\frac{\alpha_\text{L}}{\kappa_f} \text{W}_0\left(\frac{\kappa_f}{\alpha_\text{L}}\right), \frac{\alpha_\text{L}}{\kappa_f} \text{W}_0\left(\frac{\kappa_f}{\alpha_\text{L}} \left(\frac{\tau N_\text{o}}{\text{G}_{\text{m,t}}\text{G}_{\text{m,r}}\gamma}\right)^{\frac{-1}{\alpha_\text{L}}}\right)\right).$$

Proof. The SNR coverage at the typical user is given as

$$\mathbb{P}\left(\frac{S(R_\text{o})}{N_\text{o}} > \tau\right) = \mathbb{P}\left(S(R_\text{o}) > \tau N_\text{o}\right) = \mathbb{P}\left(\min\left(1, R_\text{o}^{-\alpha} \exp(-\kappa_f R_\text{o})\right) > \frac{\tau N_\text{o}}{\text{G}_{\text{m,t}}\text{G}_{\text{m,r}}\gamma}\right).$$

Simplifying the above, we get the desired result. □

TABLE II
DEFAULT VALUES OF THE SYSTEM PARAMETERS.

Parameters	Values
Frequency f and bandwidth B	0.3 THz, 250 MHz
Molecular absorption coefficient κ_f	0.005 m^{-1}
BS density λ_b	0.005 $\mathrm{BS/m}^2$
Main lobe gain of BS and user $\mathrm{G}_{\mathrm{m,t}} = \mathrm{G}_{\mathrm{m,r}}$	25 dB
Side lobe gain of BS and user $\mathrm{G}_{\mathrm{s,t}} = \mathrm{G}_{\mathrm{s,r}}$	0 dB
Scatter density λ_s	1 $\mathrm{scatters/m}^2$
Scattering coefficient S	0.5 (rough surface)
Main lobe beamwidth ϕ_q, of BS and user	30°
Noise N_o	10^{-12} W for B=250 MHz
Path loss exponent of LOS α_L	2
Effective scatterer area of scatterer A_s	10^{-2} m^2
Trasnmit power p_t	1 W

C. Mean SINR

It can be observed that due to lack of fading in THz, the coverage probability expression requires an inversion of LT and is, hence, more involved compared to expressions at lower frequencies. Note that in the latter, the presence of fading (in particular exponential fading coefficient) facilitates analysis by allowing us to express the coverage probability directly in terms of the LT of interference distribution. Motivated by this, we propose an approach which artificially introduces a dummy exponential fading variable in the mean SINR expression without changing mean SINR value which helps us directly use the LT expressions. This approach is described in details in Appendix E. Using this approach, we get the following result.

Theorem 2. *The mean SINR for the typical user in a THz cellular network is*

$$\mathbb{E}\left[\mathrm{SINR}\right] = \int_{\tau=0}^{\infty}\int_{r_\mathrm{o}=0}^{\infty}\left(\mathcal{L}_{I_\mathrm{b}|R_\mathrm{o}=r_\mathrm{o}}\left(\frac{\tau}{\mathrm{G}_{\mathrm{m,t}}\mathrm{G}_{\mathrm{m,r}}\ell(r_\mathrm{o})}\right)\times \mathcal{L}_{I_\mathrm{s}}\left(\frac{\tau}{\mathrm{G}_{\mathrm{m,t}}\mathrm{G}_{\mathrm{m,r}}\ell(r_\mathrm{o})}\right)e^{\left(-\frac{\tau N_\mathrm{o}}{\mathrm{G}_{\mathrm{m,t}}\mathrm{G}_{\mathrm{m,r}}\ell(r_\mathrm{o})}\right)}\right) f_{R_\mathrm{o}}(r_\mathrm{o})\mathrm{d}r_\mathrm{o}\mathrm{d}\tau.$$

IV. NUMERICAL RESULTS

Now, we present some numerical results obtained from the analytical expressions derived in the previous section along with corresponding simulated results. Note that unless mentioned otherwise, the parameter values are taken as per the TABLE II.

A. Impact of scatterer density on the coverage

Fig. 1 presents the SINR coverage probability as a function of threshold τ for various values of scatterer density. For the smaller values of τ, the scatterer density does not affect the coverage probability. The impact of scatterer density on the coverage probability is significant for the moderate values of τ. We also observe that coverage probability improves with decrease in the scatterer density. To observe the impact of the BS density on the coverage probability, we present the coverage probability as a function of BS density for different values of the scatterer density in Fig. 2. We can observe that densification first helps by improving the coverage. However, increasing the BS density beyond a certain value may degrade the coverage probability. This value gives the optimal BS

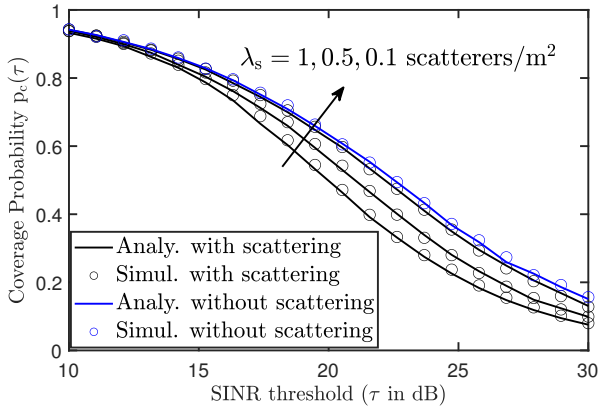

Fig. 1. Variation of the SINR coverage probability with respect to SINR threshold τ for various values of scatterer density. With an increase in the scatter density, the coverage probability reduces.

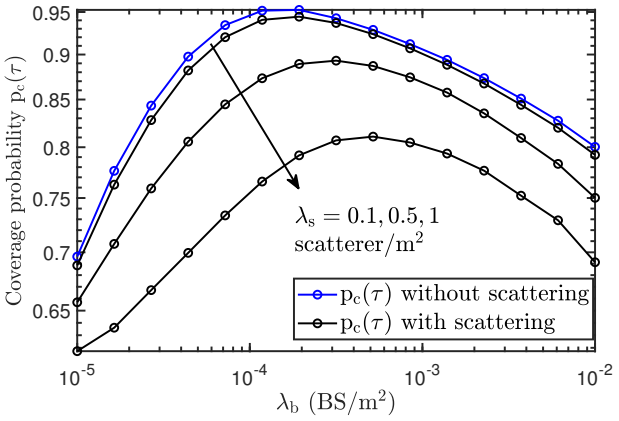

Fig. 2. The variation of coverage probability with the BS density for various values of scatterer density. Here SINR threshold $\tau = 15$ dB. There exists an optimal value of BS density, beyond which the densification may hurt the coverage.

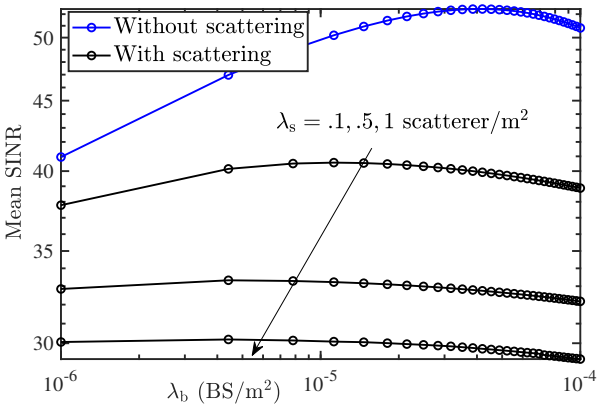

Fig. 3. The plot showing the mean SINR (in dB) with respect to BS density. It can be observed that the densification of THz BSs beyond a certain value reduces the mean SINR.

density for maximizing the coverage probability. The initial rise in coverage probability with BS density is due to increase in the signal power at the typical user. The subsequent decrease in coverage is due to increase in the number of LOS interferers. This behavior is similar to the impact of densification for mmWave networks and networks with dual slope path loss [20]. We can also observe that the impact of scatterer density is more prominent at a moderate BS density, although it affects the coverage significantly regardless of the BS density.

B. Impact of densification on the mean SINR

In Fig. 3, we present the variation of mean SINR as a function of BS density for different values of scatterer density. We can observe that the densification first increases the mean SINR. However, increasing BS density beyond a certain point degrades the mean SINR. This behavior is similar to the trends observed for coverage probability. We can also see that the mean SINR of the typical user reduces significantly with increase in the scatterer density. Further, due to interference from scatterers, the optimum BS density decreases along with the corresponding value of the optimal mean SINR. It can also be observed that if scatterers are more dense than a particular value, the mean SINR for the typical user does not improve with densification. Instead an increase in the BS density may actually hurt the mean SINR. In such scenarios, antenna alignment methods and interference cancellation may be useful for improving mean SINR.

V. Conclusion and Future Work

In this paper, we have analyzed the coverage probability and mean SINR of the typical user in the THz networks. The main technical contribution is the development of a comprehensive analytical framework that incorporates all key propagation characteristics of THz frequencies, including the effect of scattering that has been largely ignored until now. Our analysis demonstrates that the coverage probability reduces with the increase in scatterer density. We also demonstrated that the coverage probability cannot be increased indefinitely by increasing the BS density. Instead, there exists an optimal BS density, which is a function of blockage and scatterer densities. This work has several possible extensions. First, it is important to more carefully model the effect of NLOS BSs and their interplay with scattering, which we plan to do in the journal extension of this work. Second, it is important to understand the disparity in the reliabilities of different links in the network by deriving the meta distribution.

Appendix

A. Proof of Lemma 1 (LT of interference due to LOS BSs:)

Using (3) and the definition of LT [11], the LT of interference from the LOSs BS for a given R_{o} is

$$\mathcal{L}_{I_{\mathrm{b}}|R_{\mathrm{o}}}(s) = \mathbb{E}\left[e^{-sI_{\mathrm{b}}}\right]$$

$$= \mathbb{E}_{\Phi_{\mathrm{L}},\mathrm{G}_{\|\mathbf{z}_i\|}}\left[\exp\left(-s\sum_{\mathbf{z}_i\in\Phi_{\mathrm{L}},\mathbf{z}_i\neq\mathbf{z}_{\mathrm{o}}}\mathrm{G}_{z_i}\ell(\|\mathbf{z}_i\|)\right)\right]$$

$$\overset{(a)}{=} \exp\left(-2\pi\lambda_{\mathrm{b}}\sum_{n=1}^{4}\mathrm{p}_n\int_{z=R_{\mathrm{o}}}^{\infty}\left(1-e^{-s\mathrm{G}_n\ell(z)}\right)e^{-\beta z}z\mathrm{d}z\right)$$

$$\overset{(b)}{=} \exp\left(-\pi\lambda_{\mathrm{b}}R_{\mathrm{o}}^2\sum_{n=1}^{4}\mathrm{p}_n\int_{t=1}^{\infty}\left(1-e^{-s\mathrm{G}_n\ell(R_{\mathrm{o}}\sqrt{t})}\right)e^{-\beta R_{\mathrm{o}}\sqrt{t}}\mathrm{d}t\right).$$

Here, step (a) is obtained using the PGFL of PPP and (b) is obtained by substituting $z = R_{\mathrm{o}}\sqrt{t}$.

B. Proof of Lemma 2 (Average incident power on the typical scatterer:)

Without loss of generality, we assume that the typical scatterer is located at the origin. Hence, the average of total power falling on this scatterer from all the LOS BSs is

$$\mathrm{P_s} = \mathbb{E}\left[\sum_{\mathbf{z}_i\in\Phi_{\mathrm{L}}}\mathrm{p_t}g_{\mathrm{t},z_i}\frac{A_{\mathrm{s}}}{4\pi}\ell(\|z_i\|)\right]$$

$$= 2\pi\lambda_{\mathrm{b}}g_{\mathrm{t}}^1\frac{A_{\mathrm{s}}}{4\pi}\int_{z=0}^{\infty}\ell(z)e^{-\beta z}z\mathrm{d}z,$$

where $g_{\mathrm{t}}^1 = \mathrm{G_{m,t}p_t} + \mathrm{G_{s,t}}(1-\mathrm{p_t})$ is the mean of transmitting antenna gain *i.e.* $\mathbb{E}[g_{\mathrm{t}}]$.

C. Proof of Lemma 3 (LT of interference due to scatterers:)

Using (4) and the definition of LT [11], the LT of I_{s} is

$$\mathcal{L}_{I_{\mathrm{s}}}(s) = \mathbb{E}\left[e^{-sI_{\mathrm{s}}}\right] \overset{(a)}{=} \mathbb{E}\left[e^{-s\sum_{\mathbf{y}_i\in\Phi_s'}\mathrm{P_{s},}iS^2g_{\mathrm{r},y_i}\ell(y_i)}\right]$$

$$\overset{(b)}{=} \exp\left(-2\pi\lambda_s\sum_{j=1}^{2}\mathrm{p_{r},}j\int_{y=0}^{\infty}\left(1-e^{-sh_j(y)}\right)e^{-\beta y}y\mathrm{d}y\right),$$

where (a) is obtained by using (4) and we get the step (b) by using the PGFL of PPP which completes the proof.

D. Proof of Theorem 1 (Coverage probability at the typical user:)

From (6)

$$\mathrm{p_c}(\tau) = \mathbb{P}(\mathrm{SINR} > \tau) = \mathbb{P}\left(\frac{S(R_{\mathrm{o}})}{I_{\mathrm{b}}+I_{\mathrm{s}}+N_{\mathrm{o}}} > \tau\right)$$

$$= \mathbb{P}\left(S(R_{\mathrm{o}}) > \tau(I_{\mathrm{b}}+I_{\mathrm{s}}+N_{\mathrm{o}})\right).$$

Using Gil-Pelaez inversion theorem [19] and averaging over the nearest LOS BS distance R_{o}, the coverage probability can be obtained as

$$\mathrm{p_c}(\tau) = \mathbb{E}_{R_{\mathrm{o}}}\left[\frac{1}{2}-\frac{1}{\pi}\int_{u=0}^{\infty}\mathrm{Im}\left[\mathbb{E}\left[e^{-juS'}|R_{\mathrm{o}}\right]e^{ju\tau N_{\mathrm{o}}}\right]\frac{\mathrm{d}u}{u}\right], \tag{13}$$

where $S' = S(R_{\mathrm{o}}) - \tau(I_{\mathrm{b}}+I_{\mathrm{s}})$. Note that

$$\mathbb{E}\left[e^{-juS'}|R_{\mathrm{o}}\right] = \mathbb{E}\left[e^{-juS(R_{\mathrm{o}})}e^{ju\tau(I_{\mathrm{b}}+I_{\mathrm{s}})}\right].$$

Since, I_{s} is independent of nearest LOS BS distance R_{o},

$$\mathbb{E}\left[e^{-juS'}\right] = e^{-juS(R_{\mathrm{o}})}\mathcal{L}_{I_{\mathrm{b}}|R_{\mathrm{o}}}(-ju\tau)\,\mathcal{L}_{I_{\mathrm{s}}}(-ju\tau).$$

Hence,

$$
\begin{aligned}
&\mathrm{Im}\left[\mathbb{E}[e^{-juS'}]e^{ju\tau N_{\mathrm{o}}}\right]\\
&=\mathrm{Im}\left[e^{-juS(R_{\mathrm{o}})+ju\tau N_{\mathrm{o}}}\mathcal{L}_{I_{\mathrm{b}}|R_{\mathrm{o}}}(-ju\tau)\mathcal{L}_{I_{\mathrm{s}}}(-ju\tau)\right],\\
&\overset{(a)}{=}\mathrm{Im}\Bigg[e^{-juS(R_{\mathrm{o}})+ju\tau N_{\mathrm{o}}}\\
&\times\exp\left(-\pi\lambda_{\mathrm{b}}\sum_{n=1}^{4}\mathrm{p}_n\int_{t=1}^{\infty}\left(1-e^{\left(ju\tau f_n(R_{\mathrm{o}}\sqrt{t})\right)}\right)e^{-\beta R_{\mathrm{o}}\sqrt{t}}R_{\mathrm{o}}^2\mathrm{d}t\right)\\
&\times\exp\left(-2\pi\lambda_{\mathrm{s}}\sum_{j=1}^{2}\mathrm{p}_j\int_{y=0}^{\infty}\left(1-e^{ju\tau h_j(y)}\right)e^{-\beta y}y\mathrm{d}y\right)\Bigg],\\
&\overset{(b)}{=}\mathrm{Im}\Bigg[e^{-juS(R_{\mathrm{o}})+ju\tau N_{\mathrm{o}}}\exp\left(-\pi\lambda_{\mathrm{b}}\sum_{n=1}^{4}\mathrm{p}_n\int_{t=1}^{\infty}\right.\\
&\left.\left(1-\cos\left(u\tau f_n(R_{\mathrm{o}}\sqrt{t})\right)-j\sin\left(u\tau f_n(R_{\mathrm{o}}\sqrt{t})\right)\right)e^{-\beta R_{\mathrm{o}}\sqrt{t}}R_{\mathrm{o}}^2\mathrm{d}t\right)\\
&\exp\left(-2\pi\lambda_s\sum_{j=1}^{2}\mathrm{p}_j\int_{y=0}^{\infty}\left(1-\cos\left(u\tau h_j(y)\right)-j\sin\left(u\tau h_j(y)\right)\right)\right.\\
&\left.\times e^{-\beta y}y\mathrm{d}y\right)\Bigg],\\
&\overset{(c)}{=}\mathrm{Im}\Bigg[H(R_{\mathrm{o}},\tau)e^{-juS(R_{\mathrm{o}})+ju\tau N_{\mathrm{o}}}\\
&\times\exp\left(j\sum_{n=1}^{4}\mathrm{p}_n\pi\lambda_{\mathrm{b}}\int_{t=1}^{\infty}\sin\left(u\tau f_n(R_{\mathrm{o}}\sqrt{t})\right)e^{-\beta R_{\mathrm{o}}\sqrt{t}}R_{\mathrm{o}}^2\mathrm{d}t\right)\\
&\times\exp\left(j\sum_{j=1}^{2}\mathrm{p}_j2\pi\lambda_{\mathrm{s}}\int_{y=0}^{\infty}\sin(u\tau h_j(y))e^{-\beta y}y\mathrm{d}y\right)\Bigg]\\
&=-H(R_{\mathrm{o}},\tau)\sin\left(uS(R_{\mathrm{o}})-\Theta(R_{\mathrm{o}},\tau)-u\tau N_{\mathrm{o}}\right),
\end{aligned}
$$

where in step (a), $f_n(z)=\mathrm{G}_n\ell(z)$ and is obtained by substituting the LT of BS interference and scatterer interference as given in (8) and (10) respectively, step (b) due to Euler's formula, step (c) is by extracting cos terms and using definition of H and the last step is due to definition of Θ and the fact that $\mathrm{Im}[e^{jt}]=\sin(t)$ for any real t. Substituting it back in (13), we get the desired the result.

E. Proof of Theorem 2 (Mean SINR at the typical user:)

To derive the mean SINR, we introduce an artificial independent exponential RV F of unit mean. Now, define another random variable $\overline{\mathrm{SINR}}=F\times\mathrm{SINR}$. Its mean is given as

$$\mathbb{E}[\overline{\mathrm{SINR}}]=\mathbb{E}\left[F\times\mathrm{SINR}\right]=\mathbb{E}[F]\mathbb{E}[\mathrm{SINR}]=\mathbb{E}[\mathrm{SINR}].$$

This shows that multiplication by F does not change the mean of SINR. Hence,

$$
\begin{aligned}
\mathbb{E}[\mathrm{SINR}]&=\mathbb{E}[F\times\mathrm{SINR}]=\int\mathbb{P}[\mathrm{SINR}>\tau]\mathrm{d}\tau\\
&\overset{(a)}{=}\int_{\tau=0}^{\infty}\mathbb{P}\left(\frac{FS(R_{\mathrm{o}})}{I_{\mathrm{b}}+I_{\mathrm{s}}+N_{\mathrm{o}}}>\tau\right)\mathrm{d}\tau\\
&\overset{(b)}{=}\int_{0}^{\infty}\mathbb{E}\left[\exp\left(-\frac{\tau}{S(R_{\mathrm{o}})}\left(I_{\mathrm{b}}+I_{\mathrm{s}}+N_{\mathrm{o}}\right)\right)\right]\mathrm{d}\tau\\
&\overset{(c)}{=}\int_{\tau=0}^{\infty}\mathbb{E}_{R_{\mathrm{o}}}\left[\mathcal{L}_{I_{\mathrm{b}}|R_{\mathrm{o}}}(s)\exp\left(-\frac{\tau N_{\mathrm{o}}}{S(R_{\mathrm{o}})}\right)\mathcal{L}_{I_{\mathrm{s}}}(s)\right]\mathrm{d}\tau.
\end{aligned}
$$

where step (a) is obtained by substituting the value of SINR, step (b) is due to CCDF of F and step (c) is due to definition of LT. This completes the proof.

REFERENCES

[1] S. Tripathi, N. V. Sabu, A. K. Gupta, and H. S. Dhillon, "Millimeter-wave and terahertz spectrum for 6G wireless," in *6G Mobile Wireless Networks*. Springer, 2021, pp. 83–121.

[2] V. Petrov, D. Moltchanov, and Y. Koucheryavy, "Interference and SINR in dense terahertz networks," in *Proc. IEEE Veh. Technol. Conf.*, 2015.

[3] V. Petrov, M. Komarov, D. Moltchanov, J. M. Jornet, and Y. Koucheryavy, "Interference and SINR in millimeter wave and terahertz communication systems with blocking and directional antennas," *IEEE Trans. Wireless Commun.*, vol. 16, no. 3, pp. 1791–1808, March 2017.

[4] J. Kokkoniemi, J. Lehtomäki, and M. Juntti, "Stochastic geometry analysis for mean interference power and outage probability in THz networks," *IEEE Trans. Wireless Commun.*, vol. 16, no. 5, pp. 3017–3028, May 2017.

[5] D. Moltchanov, P. Kustarev, and Y. Koucheryavy, "Analytical approximations for interference and SIR densities in terahertz systems with atmospheric absorption, directional antennas and blocking," *Physical Communication*, vol. 26, pp. 21–30, Feb. 2018.

[6] J. Sayehvand and H. Tabassum, "Interference and coverage analysis in coexisting RF and dense terahertz wireless networks," *IEEE Wireless Commun. Lett.*, vol. 9, no. 10, pp. 1738–1742, Oct. 2020.

[7] A. A. Raja, H. Pervaiz, S. A. Hassan, S. Garg, M. S. Hossain, and M. Jalil Piran, "Coverage analysis of mmwave and THz-enabled aerial and terrestrial heterogeneous networks," *IEEE Trans. Intell. Transp. Syst.*, vol. 23, no. 11, pp. 22 478–22 491, Nov. 2022.

[8] A. Shafie, N. Yang, S. Durrani, X. Zhou, C. Han, and M. Juntti, "Coverage analysis for 3D terahertz communication systems," *IEEE J. Sel. Areas Commun*, vol. 39, no. 6, pp. 1817–1832, June 2021.

[9] K. Humadi, I. Trigui, W.-P. Zhu, and W. Ajib, "Coverage analysis of user-centric dense terahertz networks," *IEEE Commun. Lett.*, vol. 25, no. 9, pp. 2864–2868, Sept. 2021.

[10] T. Bai and R. W. Heath, "Coverage and rate analysis for millimeter-wave cellular networks," *IEEE Trans. Wireless Commun.*, vol. 14, no. 2, pp. 1100–1114, Feb. 2015.

[11] J. G. Andrews, A. K. Gupta, A. Alammouri, and H. S. Dhillon, *An Introduction to Cellular Network Analysis using Stochastic Geometry*. Morgan Claypool (Springer).

[12] S. Mumtaz, J. M. Jornet, J. Aulin, W. H. Gerstacker, X. Dong, and B. Ai, "Terahertz communication for vehicular networks," *IEEE Trans. Veh. Technol.*, vol. 66, no. 7, July 2017.

[13] C. Chaccour, M. N. Soorki, W. Saad, M. Bennis, and P. Popovski, "Can terahertz provide high-rate reliable low latency communications for wireless VR?" *IEEE Internet of Things Journal*, vol. 9, no. 12, pp. 9712–9729, June 2022.

[14] S. Ju, S. H. A. Shah, M. A. Javed, J. Li, G. Palteru, J. Robin, Y. Xing, O. Kanhere, and T. S. Rappaport, "Scattering mechanisms and modeling for terahertz wireless communications," in *Proc. ICC*, 2019.

[15] M. Di Renzo, "Stochastic geometry modeling and analysis of multi-tier millimeter wave cellular networks," *IEEE Trans. Wireless Commun.*, vol. 14, no. 9, pp. 5038–5057, Sept. 2015.

[16] S. K. Gupta, V. Malik, A. K. Gupta, and J. G. Andrews, "Impact of blocking correlation on the performance of mmwave cellular networks," *IEEE Trans. Commun.*, vol. 70, no. 7, pp. 4925–4939, July 2022.

[17] J. M. Jornet and I. F. Akyildiz, "Channel modeling and capacity analysis for electromagnetic wireless nanonetworks in the terahertz band," *IEEE Trans. Wireless Commun.*, vol. 10, no. 10, pp. 3211–3221, Oct. 2011.

[18] T. Bai, R. Vaze, and R. W. Heath, "Analysis of blockage effects on urban cellular networks," *IEEE Trans. Wireless Commun*, vol. 13, no. 9, pp. 5070–5083, Sept. 2014.

[19] J. Gil-Pelaez, "Note on the inversion theorem," *Biometrika*, vol. 38, no. 3-4, pp. 481–482, 1951.

[20] A. K. Gupta, N. V. Sabu, and H. S. Dhillon, "Fundamentals of network densification," in *5G and Beyond*. Springer, 2021, pp. 129–163.